We are IntechOpen, the world's leading publisher of Open Access books Built by scientists, for scientists

4,800
Open access books available

122,000
International authors and editors

135M
Downloads

Our authors are among the

154
Countries delivered to

TOP 1%
most cited scientists

12.2%
Contributors from top 500 universities

CLARIVATE ANALYTICS BOOK CITATION INDEX INDEXED

WEB OF SCIENCE™

Selection of our books indexed in the Book Citation Index in Web of Science™ Core Collection (BKCI)

Interested in publishing with us?
Contact book.department@intechopen.com

Numbers displayed above are based on latest data collected.
For more information visit www.intechopen.com

Chapter

Robust Guidance Algorithm against Hypersonic Targets

Jian Chen, Yu Han and Yuan Ren

Abstract

This chapter presents a robust guidance algorithm for intercepting hypersonic targets. Since the differential of the line-of-sight rate is more sensitive to the target maneuver, a nonlinear proportional and differential guidance law (NPDG) is given by employing the differential of the line-of-sight rate produced by a nonlinear tracking differentiator. Based on the NPDG, a fractional calculus guidance law (FCG) is presented by utilizing the differential definition of fractional order. On the basis of interceptor-target relative motions, the stability criteria of the guidance system of the FCG are deduced. In different target maneuver and noisy cases, simulation results verify that the proposed guidance laws have small miss distances and the FCG has a stronger robustness.

Keywords: hypersonic target, target maneuver, fractional order control, guidance law, stability criteria

1. Introduction

In recent years, many countries are vigorously developing hypersonic weapons in near space, such as the United States (AHW, HTV-2, X-51 and X-43), India (HSTDV and RLV-TD), China (WU-14) and Russia (GLL-31). Because of its ultra-high speed and non-fixed trajectory, the hypersonic weapon has become a great strategic threat to homeland air defense [1–5]. The hypersonic vehicle flies over 5 Mach in the near space covering distances of 20–100 km. Compared with the ballistic missile, the hypersonic weapon is usually designed in a lifting body to obtain stronger maneuverability. Traditional defense systems against cruise missiles in the atmosphere cannot reach the near space. Thereby, the near space hypersonic weapon is a threat to the current defense system.

There are mainly two kinds of hypersonic vehicles. One is the air-breathing cruise vehicle [6]. Its maneuverability is relatively weaker, thus its interception is relatively easier as its trajectory is predictable. The other is the gliding entry vehicle [7]. At the entry stage, its velocity is up to 25 Mach at maximum. In the entry phase, it is able to glide thousands of kilometers in the near space without any power. In the terminal phase, a dive attack is performed to the target on the ground [8]. Therefore, its trajectory is not predictable and its interception is a challenge. A lot of research on entry guidance techniques with no-fly zone constraints has been conducted for hypersonic weapons [9, 10]. However, there are few research works

on intercepting these vehicles [11]. Consequently, new technical challenges are raised to intercept these weapons [12].

The proportional navigation guidance law (PNG) for interception has a big disadvantage of the guidance command being behind the target maneuver [13]. Actually, PNG is a proportional controller belonging to the PID controller family. Since $\ddot{q}$ embodies the target maneuver, to add a differential part $K_D \cdot \ddot{q}$ into the PNG is reasonable. Thus, the proportional and differential (PD) controller is utilized to formulate the guidance law in a hypersonic pursuit-evasion game.

By introducing fractional calculus to PID control, the fractional order PID control has become an emerging field since the 1990s [14]. Fractional calculus is a generalization of the classical integer order calculus. There are mainly three fractional calculus definitions, including Riemann-Liouville (RL) definition, Grünwald-Letnikov (GL) definition and Caputo definition. Since the Gamma function and precise solution of fractional order equations are developed, fractional calculus has appeared in the control field [15, 16]. Like integer order PID controllers, the fractional order PID controller can also be classified into PI^{λ}, PD^{μ} and $PI^{\lambda}D^{\mu}$ (λ and μ represent fractional orders). Compared to integer order PD controller concerned in this chapter, the fractional order PD^{μ} controller has the following advantages. First, a fractional order controller has greater control flexibility. There are proportional and differential fractional order μ in the PD^{μ} controller. The selection of fractional order makes it more flexible than the integer order PD controllers. Secondly, fractional order makes the controller more robust. Fractional order controller is insensitive to the parameter uncertainties of the controller and controlled plant. Even if the system parameters change a lot, a fractional order controller can still work well.

The memory function and stability characteristic make the fractional order PID controller widely applicable in the field of aircraft guidance and control [15, 16], such as pitch loop control of a vertical takeoff and landing unmanned aerial vehicle (UAV) [17], roll control of a small fixed-wing UAV [18], perturbed UAV roll control [19], hypersonic vehicle attitude control [20], aircraft pitch control [21], deployment control of a space tether system [22], position control of a one-DOF flight motion table [23], and vibration attenuation to airplane wings [24]. The viscosity of the atmosphere interacting with air vehicles has given the aircrafts the similar aerodynamics to the fractional order systems, thus the fractional order PID control theory is appropriate to design aircraft guidance and control systems.

Han et al. designed a fractional order strategy to control the pitch loop of a vertical takeoff and landing UAV. Simulations verified that the proposed controller was superior to an integer order PI controller based on the modified Ziegler-Nichols tuning rule and a general integer order PID controller in robustness and disturbance rejection [17]. Luo et al. developed a fractional order PI^{λ} controller to control the roll channel of a small fixed-wing UAV. From both simulation and real flight experiments, the fractional order controller outperformed the modified Ziegler-Nichols PI and the integer order PID controllers [18]. Seyedtabaii applied a fractional order PID controller to the roll control of a small UAV in dealing with system uncertainties, where the aerodynamic parameters are often approximated roughly [19]. Song et al. proposed a nonlinear fractional order proportion integral derivative ($NFOPI^{\lambda}D^{\mu}$) active disturbance rejection control strategy for hypersonic vehicle flight control. The proposed method was composed of a tracking-differentiator, an $NFOPI^{\lambda}D^{\mu}$ controller and an extended state observer. Simulations showed that the proposed method made the hypersonic vehicle nonlinear model track-desired commands quickly and accurately, and it has robustness against disturbances [20]. Kumar et al. developed the fractional order PID (FOPID) and integer order PID controllers using multi-objective optimization based on the bat algorithm and differential evolution technique. The proposed controllers were applied to the aircraft

pitch control. Simulations demonstrated that the FOPID controller using multi-objective bat-algorithm optimization had better performance than others [21]. Ref. [22] proposed a fractional order tension control law for deployment control of a space tether system, and its stability was proved. Ref. [23] realized a fractional order controller for position control of a one-DOF flight motion table. The flight motion table was used for simulating the rotational movement of flying vehicles. Experiments showed that tracking of a position profile using fractional order controller was feasible in real time. Ref. [24] presented a tuning method of a fractional order proportional derivative controller based on three points of the Bode magnitude diagram for vibration attenuation. An aluminum beam replicating an airplane wing verified the proposed controller.

However, not much effort has been made to deal with the pursuit-evasion problem against target maneuver and guidance noise with the fractional order PID controller. Ye et al. presented a 3D extended PN guidance law for intercepting a maneuvering target based on fractional order PID control theory and demonstrated that the air-to-air missile had a smaller miss distance to a maneuvering target [25]. However, in their research, the velocity of the missile was twice as much as that of the target, and the noise impacting on the guidance state (such as line-of-sight rate) was not taken under consideration, which limits the proposed algorithm's practical engineering applications. For this reason, based on a nonlinear proportional and differential guidance law (NPDG) and fractional calculus technique, a fractional calculus guidance law (FCG) is proposed to intercept a hypersonic maneuverable target in this chapter. It is assumed that the velocity of the interceptor is same as that of the hypersonic target, which means the target can evade as fast as the interceptor, and the guidance noise of the line-of-sight rate is considered.

The rest of this chapter is organized as follows. Section 2 formulates the FCG and the system stability condition is given. Numerical experiments are carried out in Section 3, and Section 4 concludes this work.

2. Guidance law design

2.1 Definition of the NPDG

The PNG is given by

$$a_M(t) = K_P V_R(t)\dot{q}(t), \tag{1}$$

where $\dot{q}$ is the line-of-sight (LOS) angular rate, $a_M(t)$ is the normal acceleration command of the interceptor, $V_R(t)$ is the approaching velocity between the interceptor and the target, and K_P is the proportional coefficient.

For compensating the negative influence of the target maneuver, the LOS acceleration $\ddot{q}$ is considered. A nonlinear proportional and differential guidance law (NPDG) is presented as

$$a_M(t) = K_P V_R(t)\dot{q}(t) + K_D V_R(t)\ddot{q}(t), \tag{2}$$

where K_D is the differential coefficient.

A nonlinear tracking differentiator is used to estimate $\ddot{q}$. The state equation is given by

$$\begin{cases} \dot{x}_1 = x_2, \\ \dot{x}_2 = -K\,\mathrm{sgn}\left(\dfrac{x_1 - \dot{q}_m + |x_2|x_2}{2K}\right), \end{cases} \tag{3}$$

where K is the estimation coefficient, $\dot{q}_m(t)$ is the LOS rate measured by the seeker, $\dot{q}_m(t)$ and $\ddot{q}_m(t)$ are estimated by x_1 and x_2, namely $x_1 = \hat{\dot{q}}_m(t)$ and $x_2 = \hat{\ddot{q}}_m(t)$. It is not easy to determine the value of K. If K is larger, the estimation will be more precise and the phase lag will be less, but the estimation will be noisier. Therefore, a fractional calculus guidance law is presented.

2.2 Formulation of the FCG

The Grünwald-Letnikov (GL) fractional differential definition to formulate the FCG is presented as

$$ {}_a^G D_t^\mu f(t) = \lim_{h\to 0} \frac{1}{h^\mu} \sum_{k=0}^{\frac{t-a}{h}} (-1)^k \frac{\Gamma(\mu+1)}{k!\Gamma(\mu-k+1)} f(t-kh), \tag{4} $$

which extends it from integer order to fractional order.

On dividing the continuous interval $[a, t]$ of $f(t)$ with step h = 1, and setting $n \in \{1, 2, ..., t\text{-}a\}$, the difference equation of the fractional differential signal of $f(t)$ is given by

$$ \frac{d^\mu f(t)}{dt^\mu} \approx f(t) + (-\mu) f(t-1) + \frac{(-\mu)(-\mu+1)}{2} f(t-2) + ... + \frac{\Gamma(-\mu+1)}{n!\Gamma(-\mu+n+1)} f(t-n). \tag{5} $$

According to definitions of the NPDG and GL, the FCG is proposed as

$$ a_M(t) = K_P V_R(t) x(t) + K_D V_R(t) \frac{d^\mu x(t)}{dt^\mu}, \tag{6} $$

where μ is the fractional order, $\frac{d^\mu x(t)}{dt^\mu}$ is the fractional differential of $x(t)$, and $x(t) = \dot{q}(t)$.

In the FCG, the future state of the GL fractional differential of $\dot{q}$ depends on the previous and current states. But in the NPDG, the future state $\ddot{q}$ only depends on the current state. It indicates that the fractional order part is a filter with the "memory" characteristic. The FCG runs like a filter, which is insensitive to the noises, and shows robustness to disturbances.

2.3 Stability criteria

As shown in **Figure 1**, the target and interceptor are located in the same plane, XOY, where M and T denote the interceptor and target; θ_M and θ_T represent flight

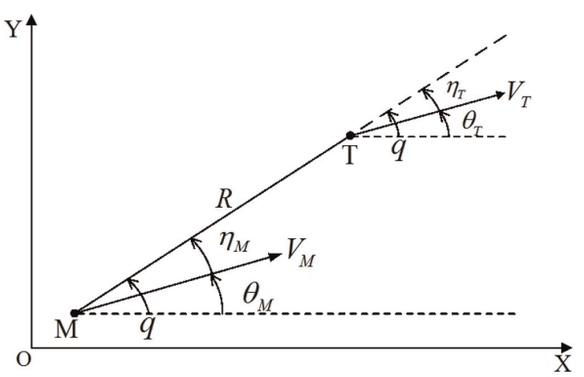

Figure 1.
Planar endgame engagement geometry.

path angles of the interceptor and target; η_M and η_T represent their heading angles; V_M and V_T represent their velocities; R represents the relative distance between them; and q is the line-of-sight angle of the interceptor.

The relative motion equations are given by

$$\dot{q} = \frac{1}{R}(V_M \sin\eta_M - V_T \sin\eta_T), \tag{7}$$

$$V_R = \dot{R} = -V_M \cos\eta_M + V_T \cos\eta_T, \tag{8}$$

$$q = \theta_M + \eta_M = \theta_T + \eta_T. \tag{9}$$

Differentiating Eq. (7), and substituting Eq. (8) and Eq. (9) into it, we have

$$R\ddot{q} + 2\dot{R}\dot{q} = \dot{V}_M \sin(\dot{q} - \dot{\theta}_M) - \dot{V}_T \sin(\dot{q} - \dot{\theta}_T) + \dot{\theta}_T V_T \cos(\dot{q} - \dot{\theta}_T) - \dot{\theta}_M V_M \cos(\dot{q} - \dot{\theta}_M). \tag{10}$$

2.3.1 Linearization

For a nonlinear problem Eq. (10), classic stability analysis theories such as the Routh-Hurwitz stability criterion for linear systems cannot be applied directly. Linearization must be done first.

Considering the practical situation, the values of $\dot{V}_M$, $\dot{V}_T$ and $\dot{\theta}_T$ will approach zero in the endgame [26]. Then, the nonlinear system Eq. (10) can be simplified into a linear system:

$$R\ddot{q} + 2\dot{R}\dot{q} \approx -\dot{\theta}_M V_M \cos(q - \theta_M). \tag{11}$$

From Eq. (11), the transfer function of the guidance system is obtained as

$$\frac{\dot{q}(s)}{\dot{\theta}_M(s)} = \frac{-V_M \cos(q - \theta_M)}{Rs + 2\dot{R}} = \frac{-K_G}{T_G - 1}, \tag{12}$$

where

$$K_G = \frac{V_M \cos(q - \theta_M)}{2|\dot{R}|}, T_G = \frac{R}{2|\dot{R}|}.$$

Thus, we get

$$\dot{q}(s) = \frac{-K_G}{T_G s - 1}\dot{\theta}_M(s). \tag{13}$$

From Eq. (6), since $a_M = V_M\dot{\theta}_M$, we have

$$\dot{\theta}_M = \frac{V_R}{V_M}(K_P\dot{q} + K_D\dot{q}s^{\mu}). \tag{14}$$

Substituting Eq. (14) into Eq. (13), the characteristic equation of the fractional calculus guidance system becomes

$$\frac{V_R}{V_M}K_G K_D s^{\mu} + T_G s + \left(\frac{V_R}{V_M}K_G K_P - 1\right) = 0. \tag{15}$$

2.3.2 Stability analysis

In stability analysis of Eq. (15), the Hurwitz stability criterion is appropriate to be employed.

Lemma 1: Hurwitz stability criterion [27]

For an nth-degree polynomial characteristic equation:

$$D(s) = a_0 s^n + a_1 s^{n-1} + \cdots + a_{n-1} s + a_n = 0 \ (a_0 > 0) \tag{16}$$

the necessary and sufficient stability condition, of system (16), is

$$\Delta_1 = a_1 > 0, \ \Delta_2 = \begin{vmatrix} a_1 & a_3 \\ a_0 & a_2 \end{vmatrix} > 0, \ \Delta_3 = \begin{vmatrix} a_1 & a_3 & a_5 \\ a_0 & a_2 & a_4 \\ 0 & a_1 & a_3 \end{vmatrix} > 0, \ \cdots, \Delta_n > 0. \tag{17}$$

That is, the order of principal minor determinants and the main determinant of the system (16) is positive.

Thus, based on the Hurwitz stability criterion, the necessary and sufficient stability condition of system (15) becomes

$$a_0 = \frac{V_R}{V_M} K_G K_D > 0, \tag{18}$$

$$\Delta_1 = a_1 = T_G > 0, \tag{19}$$

$$\Delta_2 = \begin{vmatrix} a_1 & a_3 \\ a_0 & a_2 \end{vmatrix} = \begin{vmatrix} T_G & 0 \\ \frac{V_R}{V_M} K_G K_D & \frac{V_R}{V_M} K_G K_P - 1 \end{vmatrix} = T_G \times \left(\frac{V_R}{V_M} K_G K_P - 1 \right) > 0. \tag{20}$$

That is

$$\begin{cases} \frac{V_R}{V_M} K_G K_D > 0, \\ T_G > 0, \\ \frac{V_R}{V_M} K_G K_P - 1 > 0. \end{cases} \tag{21}$$

Since $K_P > 0$ and $K_D > 0$, K_P can be preset as 4. As a consequence, we have $\cos(q\text{-}\theta_M) > 0.5$, that is $\cos\eta_M > 0.5$. It concludes

Theorem 1: When the interceptor's heading angle η_M is in the range of −60° to +60°, the fractional calculus guidance system remains stable.

3. Numerical simulations

3.1 Simulations design

For intercepting a hypersonic weapon, a space-based surveillance satellite and a ground-based X band radar or a marine X band radar should detect the target as early as possible to provide the interceptor enough time to launch from the ground or the aerial carrier. In the terminal phase of a hypersonic weapon, its velocity is too high to be intercepted. For example, the speed of a gliding entry vehicle is up to 25 Mach at maximum during a dive attack to the ground target. Thus, the interception

is usually designed in the gliding or cruising phase in the near space of a hypersonic weapon before its terminal phase (i.e., before a dive attack happens); then, the interceptor-target initial position and encounter condition is designed to be a head-to-head encounter. In the gliding or cruising phase in the near space of a hypersonic weapon, its velocity is relatively low (about 5 Mach), and its maneuvering amplitude cannot exceed 5 g due to the reduced aerodynamic efficiency since the atmosphere is thin in the near space, but the time instant that the hypersonic weapon starts maneuvering is flexible and adjustable for evading the interceptor's pursuit. Our preliminary studies and experiments show that it is not good for the hypersonic weapon to start maneuvering as early as possible during a pursuit-evasion game, and it is better for the hypersonic weapon to start maneuvering when the interceptor is close to it in the endgame. For the maneuvering mode of the hypersonic weapon to evade the interceptor's pursuit, the step maneuver and square maneuver are preferred to the ramp maneuver and sine maneuver since they can provide the hypersonic weapon the maximum evading acceleration instantly.

Based on the above analysis, the simulation parameters for a hypersonic pursuit-evasion game are set as: the interceptor-target initial position and heading condition is planned in a head-to-head engagement, and the initial relative distance R = 30,000 m, V_T = 5 Mach, which is along the negative X-axis; V_M = 5 Mach, and its initial direction is aimed at the target, that is $\theta_M = q$; the initial LOS angle q is 10°; the interceptor's maximum normal acceleration is 15 g; μ is set to the best value of 0.5 based on experience. Obviously, $\eta_M = q - \theta_M = 0° \in [-60°, 60°]$. The fractional calculus guidance system is stable based on Theorem 1.

According to authentic maneuvering characteristics of a hypersonic weapon in the gliding or cruising phase in the near space when the interceptor is close to it, its maneuver equations are given by.

Case 1: Step maneuver

$$a_T = 5\text{g}, \quad t \geq 8\text{s}, \tag{22}$$

Case 2: Square maneuver

$$a_T = \begin{cases} 5\text{g}, & t \in [2k+6, 2k+7)\text{s}, \\ -5\text{g}, & t \in [2k+7, 2k+8)\text{s}, \end{cases} \tag{23}$$

where a_T is the norm acceleration of the target, t is the time index and $k \in \mathbb{N}$. The target maneuvers are shown in **Figures 2** and **3**.

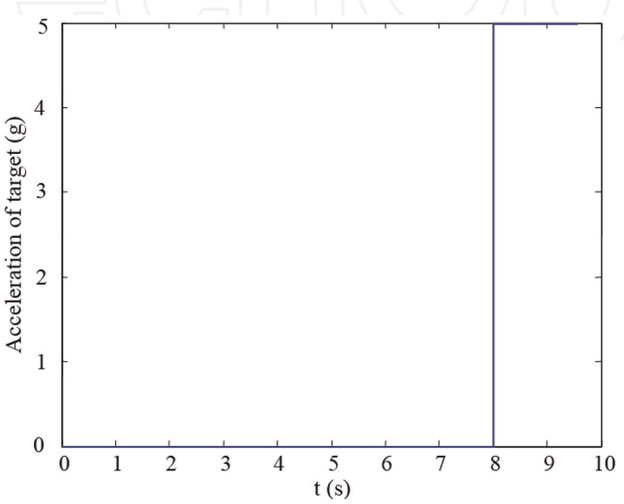

Figure 2.
Step maneuver of the target (case 1).

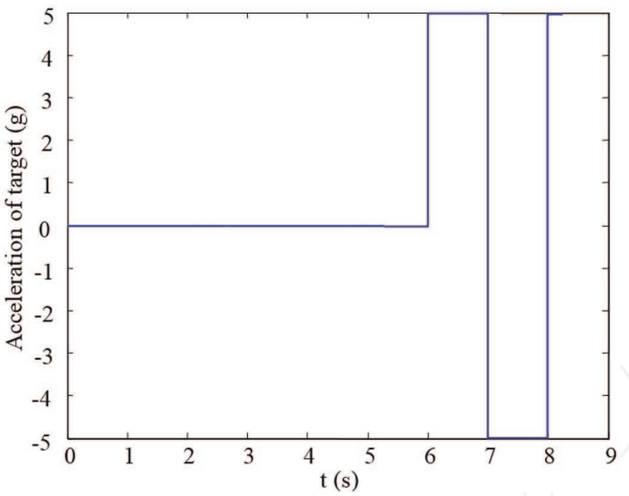

Figure 3.
Square maneuver of the target (case 2).

3.2 Interception accuracy

The trajectories, line-of-sight rates and guidance commands of the interceptor and target are shown in **Figures 4–9**. From **Figures 4** and **5**, since the velocities of the interceptor and target are hypersonic (5 Mach), the amplitude of the target maneuvers is 5 g which cannot change the velocities and trajectories of the target a lot in a limited endgame time. Thus, there is no big difference between the trajectories of the target between **Figures 4** and **5**. From **Figures 6** and **7**, the line-of-sight rates constrained by the FCG are much smaller than those constrained by the NPDG. And the line-of-sight rates of the NPDG are always non-convergent. From **Figures 8** and **9**, the guidance commands of the FCG are much smoother than those of the NPDG, which are more appropriate for the interceptor's autopilot to track. The reason is that the NPDG uses a nonlinear tracking differentiator Eq. (3) to estimate $\ddot{q}$. In Eq. (3), K is the coefficient of the estimator. The larger the K is, the more precise the estimation is and the less the phase lag is, but the noisier the

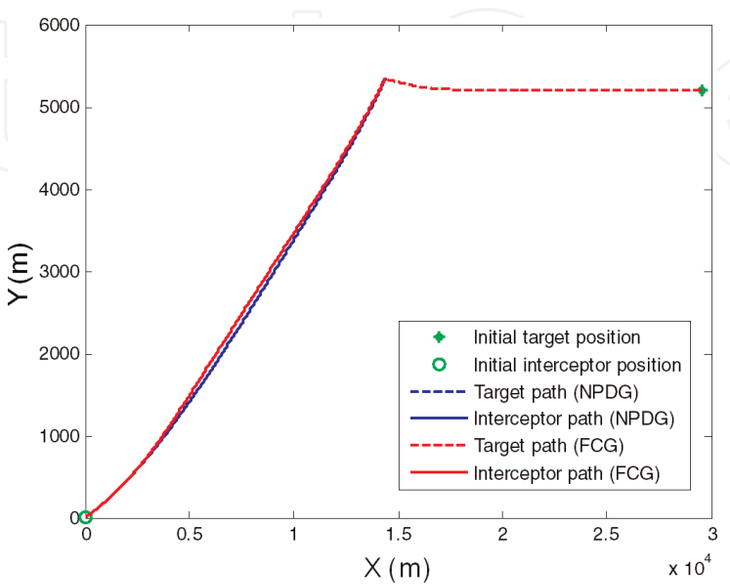

Figure 4.
Trajectories of the interceptor and target (case 1).

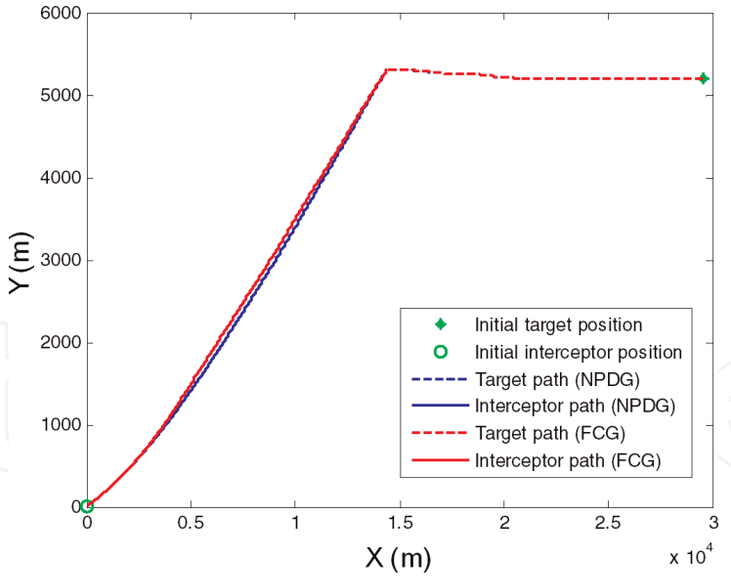

Figure 5.
Trajectories of the interceptor and target (case 2).

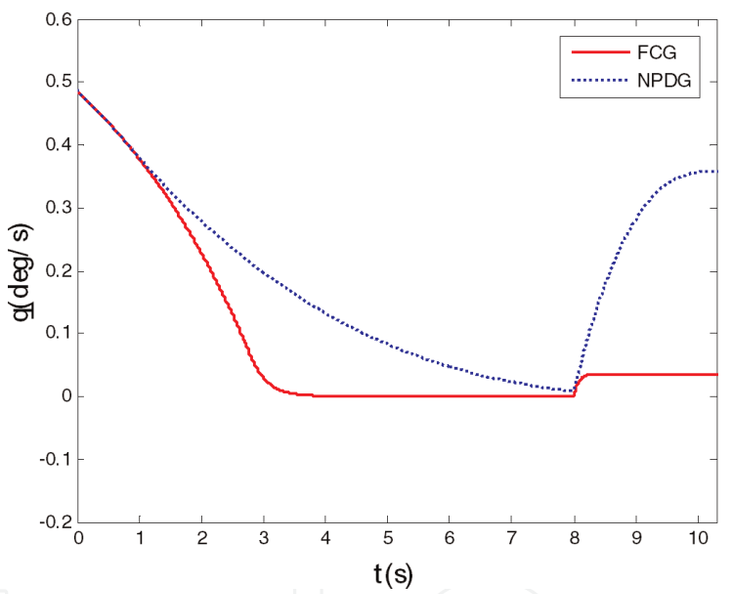

Figure 6.
Line-of-sight rates (case 1).

estimation is. Comparing **Figure 9** with **Figure 8**, the guidance command of the NPDG in case 2 is noisier than that in case 1, which means the target maneuver of case 2 is more challenging to the NPDG than that of case 1. It is also validated by the results in **Table 1** that the miss distance of the NPDG in case 2 is larger than that of the NPDG in case 1. However, the target maneuver of case 2 has little influence on the interception accuracy of the FCG, since the miss distance of the FCG in case 2 is even smaller than that of the FCG in case 1, which indicates the superiority of the FCG.

Numerical results are demonstrated in **Table 1**. The FCG has the minimum miss distance under different scenarios. In case 1, the miss distance of the FCG is 0.0322 m, which is 91% less than that of the NPDG (0.3406 m). In case 2, the miss distance of the FCG is 0.0294 m, which is 93% less than that of the NPDG (0.4151 m).

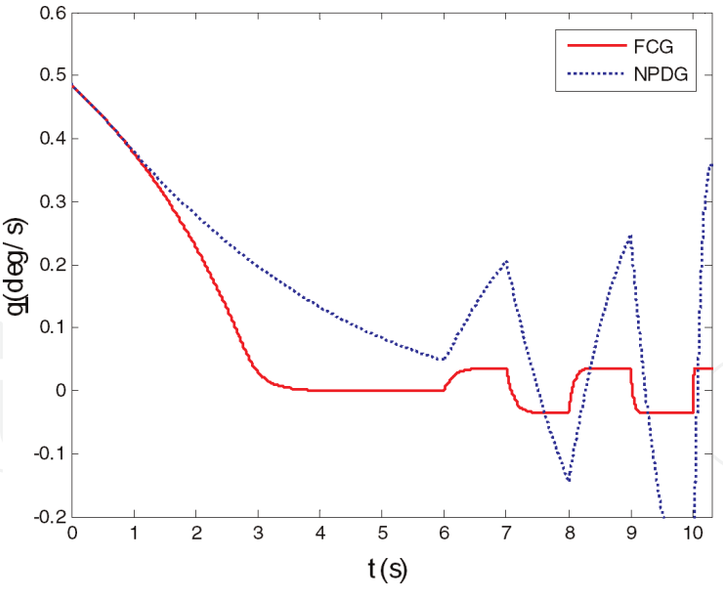

Figure 7.
Line-of-sight rates (case 2).

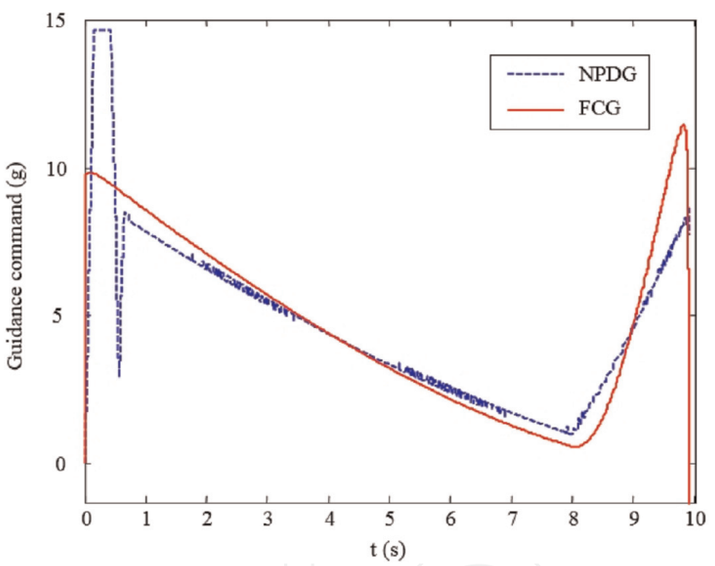

Figure 8.
Guidance commands (case 1).

3.3 Stability

In case 1, when pre-setting the simulation parameters, if the initial flight path angle θ_M is set as 40°, 70° and 75°, and other parameters remain unchanged, obviously, the heading angle $\eta_M = q - \theta_M$, will be −30°, −60° and −65°, respectively. The stabilities of the fractional calculus guidance system with the FCG can be analyzed based on Theorem 1.

As shown in **Figures 10–12**, when the heading angle ηM belongs to the closed interval [−60°, 60°], the interceptor can hit and kill the target; when the heading angle ηM is beyond the closed interval [−60°, 60°], the interception mission fails.

Simulation results are compared and summarized in **Table 2**. The miss distances increase as the heading angle goes beyond the closed interval [−60°, 60°]; when the heading angle η_M is −60°, it is a critical condition. The experimental results in **Table 2** validate the conclusion of Theorem 1.

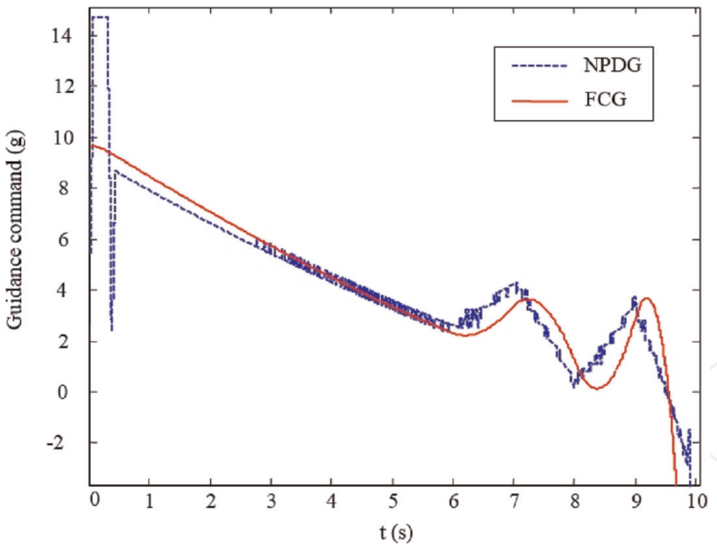

Figure 9.
Guidance commands (case 2).

Guidance law	Case 1: miss distance (m)	Case 2: miss distance (m)
NPDG	0.3406	0.4151
FCG	0.0322	0.0294

Table 1.
Performance evaluation of guidance laws.

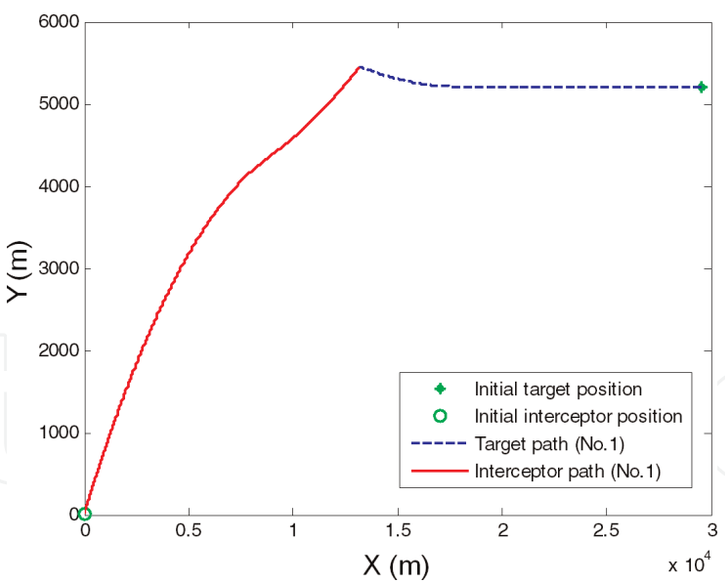

Figure 10.
Trajectories of the interceptor and target (No. 1 $\eta_M = -30°$).

3.4 Robustness

In case 1, three white noises are added into $\dot{q}$ to run 50 groups of the Monte Carlo simulations, including the amplitudes of 0.5°/s, 1.5°/s and 2.5°/s. The total number of tests is 50. The miss distance distributions of the NPDG and the FCG with a noise of 0.5°/s, 1.5°/s and 2.5°/s are shown in **Figures 13–18**.

From **Figures 13, 15** and **17**, it can be seen that the miss distances of the NPDG obviously increase as the noise increases. Similarly, from **Figures 14, 16** and **18**, the

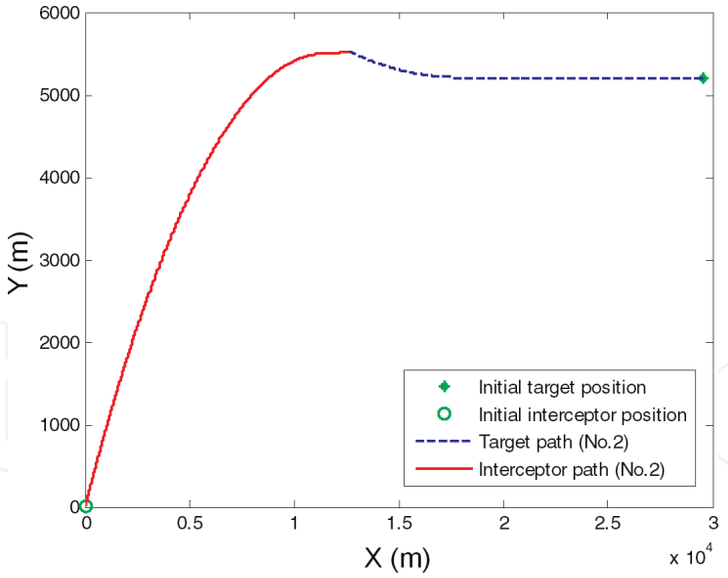

Figure 11.
Trajectories of the interceptor and target (No. 2 $\eta_M = -60°$).

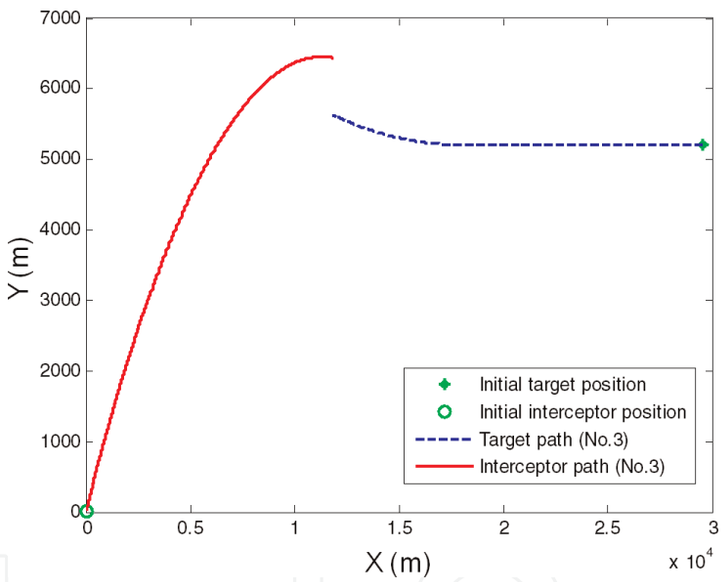

Figure 12.
Trajectories of the interceptor and target (No. 3 $\eta_M = -65°$).

No.	Heading angle η_M (°)	Stability	Miss distance (m)
1	−30	Stable	0.1060
2	−60	Stable	8.9125
3	−65	Unstable	820.7977

Table 2.
Stability analysis.

miss distances of the FCG slightly increase as the noise increases. These phenomena indicate the effect of noise impacting on the miss distances of both the NPDG and the FCG. Moreover, comparing **Figure 14** with **Figure 13**, comparing **Figure 16** with **Figure 15**, and comparing **Figure 18** with **Figure 17**, the miss distances of the

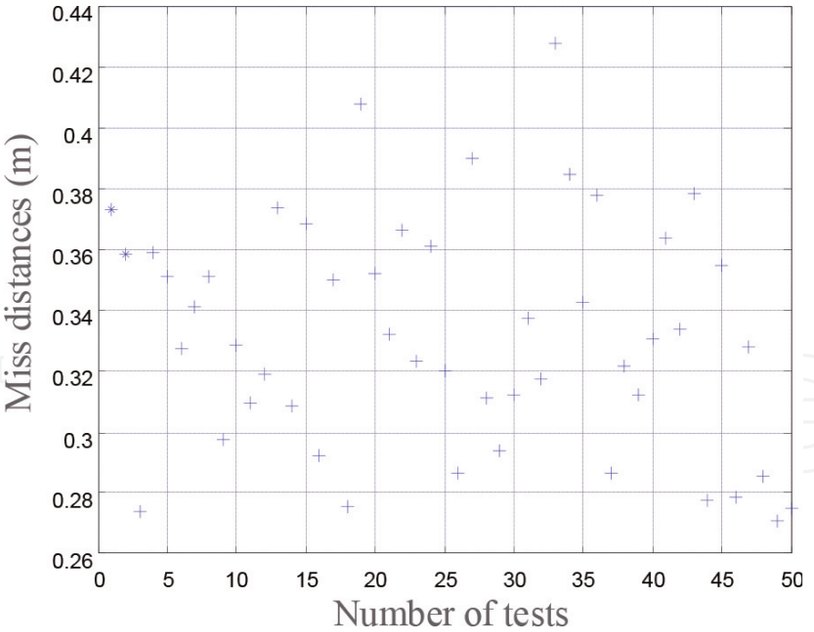

Figure 13.
Miss distance distribution of the NPDG with a noise of 0.5°/s.

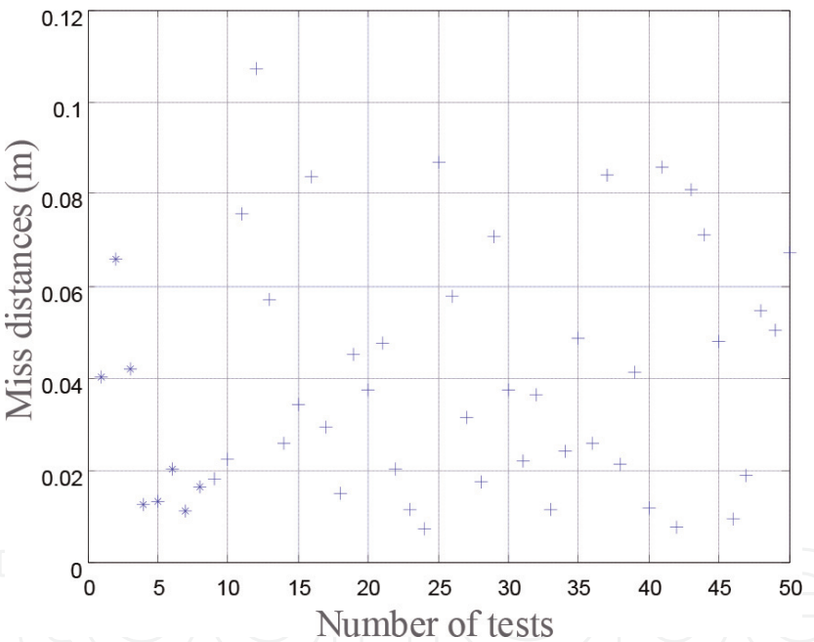

Figure 14.
Miss distance distribution of the FCG with a noise of 0.5°/s.

FCG are always smaller than those of the NPDG, which indicates the stronger robustness of the FCG.

Statistical results are indicated in **Table 3**. Obviously, compared with the NPDG, the FCG has a better robustness to the guidance noises.

To summarize the interception accuracy and robustness experiments, a conclusion can be drawn. The unique filtering properties of the fractional calculus guidance law make its interception accuracy and robustness better. For intercepting a hypersonic weapon, introducing the differential signal of the line-of-sight rate as the guidance information can effectively suppress the target maneuvers, and it has a good robustness, which can make it a feasible guidance strategy. The specifications are as follows:

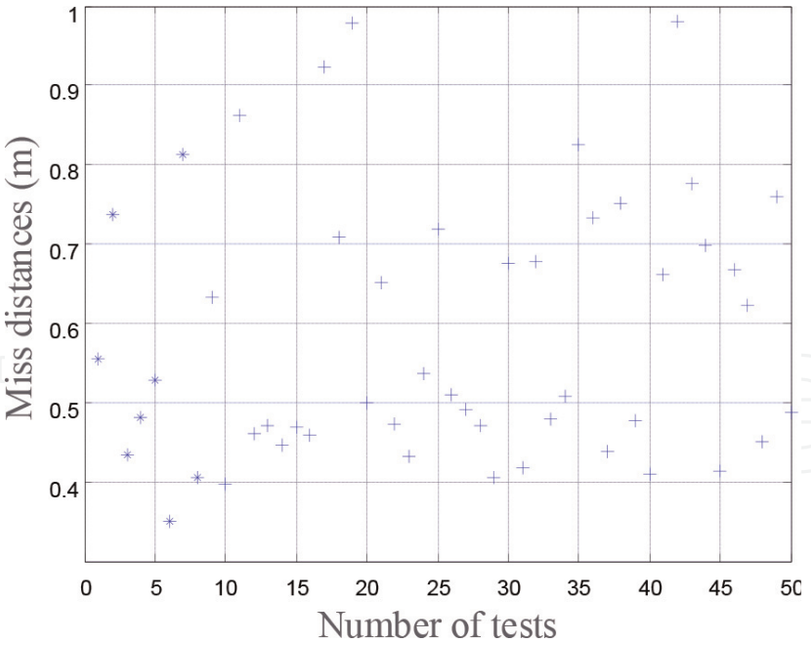

Figure 15.
Miss distance distribution of the NPDG with a noise of 1.5°/s.

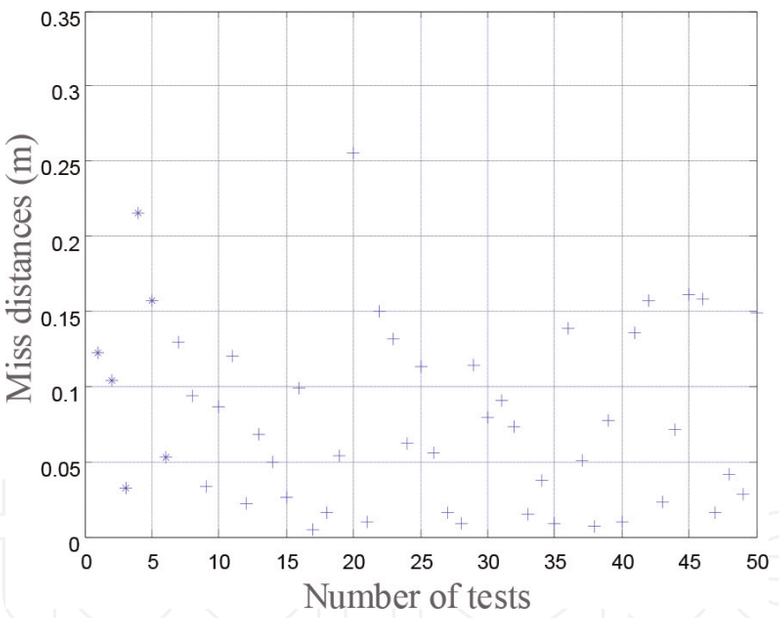

Figure 16.
Miss distance distribution of the FCG with a noise of 1.5°/s.

1. The FCG can improve the guidance accuracy. Compared with the NPDG, it has a better feasibility, since the NPDG requires the measurement of $\ddot{q}$, while this angular acceleration usually cannot be directly measured by the interceptor's seeker.

2. The robustness of the FCG is better than that of the NPDG. The FCG using the fractional differential of $\dot{q}$ improves the precision of the estimation. The filtering capability of the fractional order part in the FCG provides good stability to the system in a hypersonic pursuit-evasion game under noisy conditions.

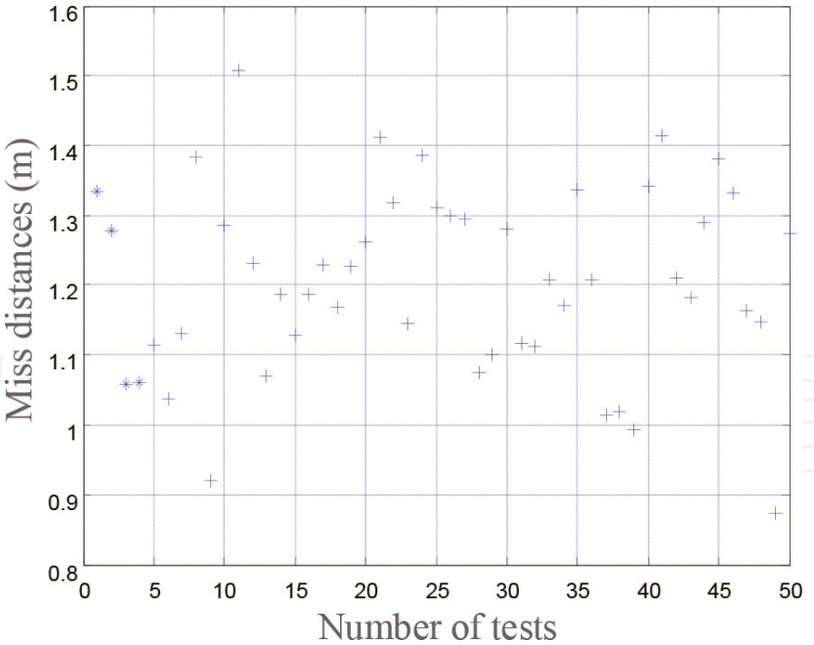

Figure 17.
Miss distance distribution of the NPDG with a noise of 2.5°/s.

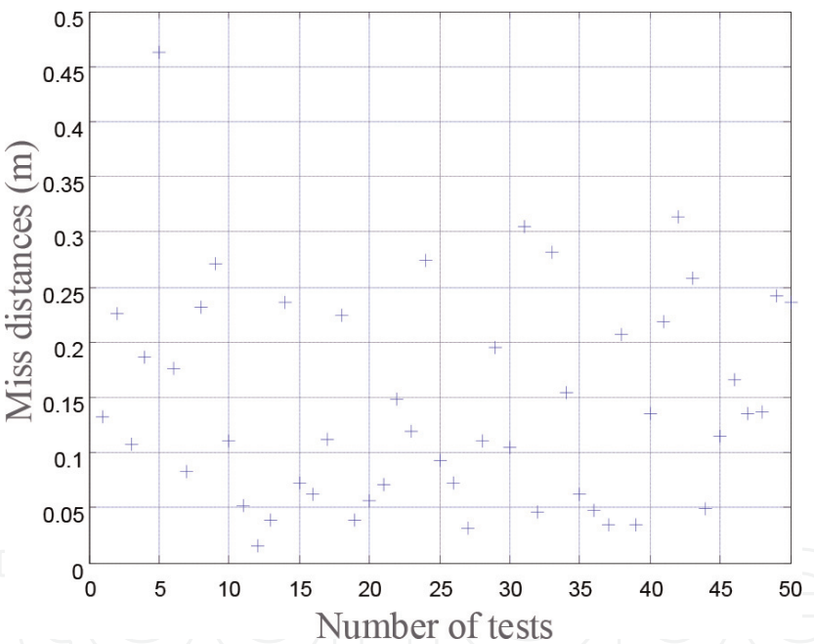

Figure 18.
Miss distance distribution of the FCG with a noise of 2.5°/s.

Noise (°/s)	Guidance law	Expectation (m)	Variance (m)
0.5	FCG	0.0396	6.7768e−004
0.5	NPDG	0.3322	0.0014
1.5	FCG	0.0786	0.0036
1.5	NPDG	0.5842	0.0274
2.5	FCG	0.1457	0.0091
2.5	NPDG	1.0092	0.2044

Table 3.
Statistical results of the miss distances under noisy conditions.

4. Conclusions

This chapter first discusses how to solve the problem of intercepting the hypersonic maneuvering target without greatly increasing the complexity degree of the guidance system. Based on the axiom that the response to the target maneuver of the differential signal of the line-of-sight rate is faster than that of the line-of-sight rate, a nonlinear proportional and differential guidance law is designed using the differential derivative of the line-of-sight rate. Based on the differential definition of fractional calculus, a fractional calculus guidance law is designed on the basis of the NPDG. In the simulation experiments of interception accuracy and robustness, both the NPDG and the FCG demonstrate guaranteed guidance performances. The influence of noises impacting on the guidance system is studied. Both of the guidance laws can effectively intercept hypersonic maneuvering targets while reducing the impact of noise signals. Furthermore, the method obtaining the fractional differential signal of $\dot{q}$ in the FCG is better than the method estimating the $\ddot{q}$ in the NPDG.

In conclusion, under the premise of not greatly increasing the complexity degree of the guidance system, introducing the differential signal of the line-of-sight rate to formulate the novel guidance laws can help meet the precision needed to intercept a hypersonic weapon. The FCG is superior to the NPDG in interception accuracy and robustness to guidance noises.

Acknowledgements

This work is supported by National Key R&D Program of China (Grant Nos. 2016YFC0400207, 2017YFD0701003 from 2017YFD0701000, and 2016YFD0200702 from 2016YFD0200700), the Jilin Province Key R&D Plan Project 2017YFD0701000, and 2016YFD0200702 from 2016YFD0200700), the Jilin (Grant Nos. 20180201036SF and 20170204008SF), and the Chinese Universities Scientific Fund (Grant Nos. 10710301, 1071-31051012, 1071-31051361, and 2019TC108).

Conflict of interest

The authors declare no conflict of interest.

Author details

Jian Chen[1,2], Yu Han[3*] and Yuan Ren[4]

1 College of Engineering, China Agricultural University, Beijing, China

2 Beijing Key Laboratory of Optimized Design for Modern Agricultural Equipment, Beijing, China

3 College of Water Resources and Civil Engineering, China Agricultural University, Beijing, China

4 Space Engineering University, Beijing, China

*Address all correspondence to: yhan@cau.edu.cn

References

[1] Romaniuk S, Grice F. The Future of US Warfare. New York: Taylor & Francis; 2017

[2] Besser H, Huggins M, Zimper D, Goge D. Hypersonic vehicles: State-of-the-art and potential game changers for future warfare. In: Brochure of 2016 NATO Science & Technology Symposium; March 2016; Brussels. Paris: NATO Science & Technology Organization; 2016. DOI: 10.13140/RG.2.1.3360.8566

[3] Majumdar S. BrahMos: A hypersonic future? Vayu Aerospace and Defence Review. 2017;**1**:116

[4] Butt Y. A hypersonic nuclear war is coming. New Perspectives Quarterly. 2016;**33**(1):51-54

[5] Bartles C. Russian threat perception and the ballistic missile defense system. Journal of Slavic Military Studies. 2017; **30**(2):152-169

[6] Murugan T, De S, Thiagarajan V. Validation of three-dimensional simulation of flow through hypersonic air-breathing engine. Defence Science Journal. 2015;**65**(4):272-278

[7] Li G, Zhang H, Tang G. Maneuver characteristics analysis for hypersonic glide vehicles. Aerospace Science and Technology. 2015;**43**:321-328

[8] Xie D, Wang Z, Zhang W. A new strategy of guidance command generation for re-entry vehicle. Defence Science Journal. 2013;**63**(1):93-100

[9] Wang T, Zhang H, Tang G. Predictor-corrector entry guidance with waypoint and no-fly zone constraints. Acta Astronautica. 2017;**138**:10-18

[10] He R, Liu L, Tang G, Bao W. Rapid generation of entry trajectory with multiple no-fly zone constraints. Advances in Space Research. 2017; **60**(7):1430-1442

[11] Liu C, Liu C, Tuan P. Algorithm of impact point prediction for intercepting reentry vehicles. Defence Science Journal. 2016;**56**(2):129-146

[12] Vathsal S, Sarkar A. Current trends in tactical missile guidance. Defence Science Journal. 2005;**55**(2):265-280

[13] Tyan F. Analysis of general ideal proportional navigation guidance laws. Asian Journal of Control. 2016;**18**(3): 899-919

[14] Das S. Functional Fractional Calculus. Berlin: Springer; 2011

[15] Chen Y, Vinagre B, Xue D. Fractional-Order Systems and Controls: Fundamentals and Applications. London: Springer; 2010

[16] Li Z, Liu L, Dehghan S, Chen Y, Xue D. A review and evaluation of numerical tools for fractional calculus and fractional order controls. International Journal of Control. 2017;**90**(6): 1165-1181

[17] Han J, Di L, Coopmans C, Chen Y. Pitch loop control of a VTOL UAV using fractional order controller. Journal of Intelligent & Robotic Systems. 2014;**73** (1–4):187-195

[18] Luo Y, Chao H, Di L, Chen Y. Lateral directional fractional order $(PI)^{\alpha}$ control of a small fixed-wing unmanned aerial vehicles: Controller designs and flight tests. IET Control Theory and Applications. 2011;**5**:2156-2167

[19] Seyedtabaii S. New flat phase margin fractional order PID design: Perturbed UAV roll control study. Robotics and Autonomous Systems. 2017;**96**:58-64

[20] Song J, Wang L, Cai G, Qi X. Nonlinear fractional order proportion integral derivative active disturbance rejection control method design for hypersonic vehicle attitude control. Acta Astronautica. 2015;**111**:160-169

[21] Kumar P, Narayan S, Raheja J. Optimal design of robust fractional order PID for the flight control system. International Journal of Computer Applications. 2015;**128**(14):31-35

[22] Sun G, Zhu Z. Fractional-order tension control law for deployment of space tether system. Journal of Guidance, Control, and Dynamics. 2014;**37**(6):2057-2061

[23] Zarei M, Arvan M, Vali A, Behazin F. Design and implementation of fractional order controller for a one DOF flight motion table. In: Proceedings of the 36th Chinese Control Conference; 26–28 July 2017; Dalian. New York: IEEE; 2017. pp. 11395-11400

[24] Birs I, Folea S, Muresan C. An optimal fractional order controller for vibration attenuation. In: Proceedings of the 25th Mediterranean Conference on Control and Automation; 3–6 July 2017; Valletta. New York: IEEE; 2017. pp. 2473-3504

[25] Ye J, Lei H, Li J. Novel fractional order calculus extended PN for maneuvering targets. International Journal of Aerospace Engineering. 2017: 5931967-1-5931967-9

[26] Ben-Asher J, Speyer J. Games in aerospace: Homing missile guidance. In: Basar T, Zaccour G, editors. Handbook of Dynamic Game Theory. Cham: Springer; 2017. pp. 1-28. DOI: 10.1007/978-3-319-27335-8_25-1

[27] Dorf R, Bishop R. Modern Control Systems. Boston: Pearson; 2011